European Journal of Neuroscience, Vol. 23, pp. 1301–1310, 2006 doi:10.1111/j.1460-9568.2006.04652.x

The preoptic hypothalamus and basal forebrain play opposing roles in the descending modulation of sleep and wakefulness in infant rats

Ethan J. Mohns, Karl Æ. Karlsson* and Mark S. Blumberg
Program in Behavioral and Cognitive Neuroscience, Department of Psychology, University of Iowa, Iowa City, IA 52242, USA

Keywords: atonia, development, modafinil, neurophysiology, rapid eye movement

Abstract

Recent findings in infant rats suggest that the preoptic area (POA) and/or basal forebrain (BF) contribute to developmental changes in sleep and wake organization between postnatal day 2 (P2) and P9. To examine the contributions of these forebrain areas to sleep and wakefulness, separate lesions of the POA or BF, or combined lesions (POA + BF), were performed at P9, and precollicular transections were performed at P2. In addition, modafinil, a drug of unknown mechanism of action the effects of which on sleep and wakefulness have been hypothesized to result from inhibition of POA activity, was administered at P2 and P9. Finally, extracellular neuronal activity was recorded from the POA and BF. POA lesions decreased sleep bout durations and increased wake bout durations. BF lesions inhibited sleep bout durations to a lesser extent, while leaving wake bout durations unaffected. POA + BF lesions produced a combination of these effects, resulting in short bouts of sleep and wakefulness similar to those of transected P8 rats. Even at P2, transections decreased sleep bout durations. The finding, however, that the sleep-inhibiting and wake-promoting effects of modafinil were more potent at P9 than at P2 suggests increasing sleep–wake modulation by the POA between these two ages. Finally, neuronal recordings confirmed the presence of state-dependent neurons within the infant POA and BF. We propose that the POA, in addition to promoting sleep, inhibits wakefulness via direct and indirect inhibitory connections with wake-promoting neurons in the BF, and that this inhibitory influence increases across early development.

Introduction

Altricial infant mammals cycle rapidly between bouts of sleep and wakefulness. Although a more consolidated sleep–wake pattern emerges gradually after birth, the neural substrates responsible for this consolidation remain unknown (Kleitman & Engelmann, 1953; Gramsbergen *et al*., 1970). In a recent study (Karlsson *et al*., 2004), it was demonstrated that transections placed caudal to the preoptic area (POA) and rostral to the midbrain (hereafter referred to as precollicular transections) in 8-day-old [postnatal day (P)8] rats resulted in rapid sleep–wake cycles similar to those of normal P2 rats. By contrast, transections rostral to the POA had no effect, thereby ruling out a contribution of more rostral structures at this age. Based on these results, it appears that the areas implicated in the developmental transition from P2 to P8 sleep–wake cyclicity include sleep- and wake-promoting regions within the POA and basal forebrain (BF) (Szymusiak, 1995; Sherin *et al*., 1996; Jones, 2003).

The POA consists primarily of three hypothalamic regions: the medial POA (MPO), the lateral POA (LPO) and the ventrolateral POA (VLPO). The POA sends inhibitory GABAergic projections to caudal wake- and rapid eye movement (REM)-active nuclei – including the tuberomammillary nucleus (TMN), dorsal raphe nucleus, locus coeruleus, and the laterodorsal and pedunculopontine tegmental nuclei – thereby promoting sleep by suppressing wakefulness (McGinty & Szymusiak, 2000; Saper *et al*., 2001). In addition, these efferent nuclei project back to the POA (Chou *et al*., 2002) and modulate its activity (Gallopin *et al*., 2000). The BF is composed of a number of forebrain nuclei, extending caudolaterally from the medial septum to the ventral pallidum (VP), and projects reciprocally to the same wake-promoting nuclei as the POA (Semba, 2000; Zaborszky & Duque, 2003). Finally, the POA and BF project to each other (Grove, 1988; Sherin *et al*., 1998; Chou *et al*., 2002).

The purpose of the present study was to investigate the individual and combined contributions of the POA and BF to the developmental changes in sleep and wakefulness during infancy. In P8–10 (hereafter referred to as P9) rats, electrolytic lesions were produced in the POA, BF or POA + BF, and bouts of sleep and wakefulness were recorded. Next, precollicular transections were performed at P2 for comparison with the effects of similar transections in older pups (Karlsson *et al*., 2004). In addition, to investigate the possibility that the POA's modulatory effects on sleep and wakefulness change across early development, modafinil was administered at both P2 and P9; although modafinil's wake-promoting mechanisms are not completely understood, the drug has been shown to potentiate the inhibition of GABAergic POA neurons *in vitro* (Gallopin *et al*., 2004). Finally, given persistent doubts concerning the brain's role in the control of

Correspondence: Dr M. S. Blumberg, as above.
E-mail: mark-blumberg@uiowa.edu

**Present address*: Program in Biomedical Engineering, Department of Science and Engineering, Reykjavik University, Reykjavik, Iceland.

Received 21 July 2005, revised 21 December 2005, accepted 23 December 2005

sleep and wakefulness in early infancy (Frank & Heller, 2003), it was important here to determine whether state-dependent neural activity can be detected within the POA and BF at P9.

Materials and methods

All experiments were carried out in accordance with the National Institutes of Health Guide for the Care and Use of Laboratory Animals (NIH Publication no. 80-23) and were approved by the Institutional Animal Care and Use Committee of the University of Iowa. All efforts were made to minimize the number of animals used.

Subjects

Twenty-one P2 and 68 P9 male Sprague–Dawley Norway rats (*Rattus norvegicus*) from 76 litters were used. When littermates were used, they were always assigned to different experimental groups. Body weights ranged from 6.5 to 9.4 g at P2 and 17.0 to 26.3 g at P9. Litters were culled to eight pups within 3 days after birth (day of birth = day 0). Mothers and their litters were housed in standard laboratory cages (48 × 20 × 26 cm) in the animal colony at the University of Iowa; food and water were available *ad libitum*. All subjects were maintained on a 12-h light/dark schedule with lights on at 07:00 h, and all tests were conducted during the lights-on phase between 12:00 and 17:00 h to minimize the possibility of circadian effects.

Brain lesions in P9 rats

Surgery

Fifty P9 rats from 50 litters were used (body weights 17.0–26.3 g). Under isoflurane anesthesia, subjects were placed in a stereotaxic apparatus (David Kopf Instruments, Tujunga, CA, USA). An insulated tungsten concentric bipolar electrode (1 MΩ, 3–4 μm at the tip, model TM33CCINS, World Precision Instruments, Sarasota, FL, USA) was lowered into the target structure under stereotaxic guidance. Coordinates for bilateral POA lesions ($n = 24$) were AP −0.7 to 1.0 mm from bregma, ML ±1.0 mm and −6.7 mm ventral to the meningeal surface. Coordinates for bilateral BF lesions ($n = 11$) were AP −0.7 mm from bregma, ML ±2.0–3.0 mm and −6.7 mm ventral to the meningeal surface. Subjects in the POA + BF ($n = 10$) group each received a total of four lesions to ablate both the POA and the BF bilaterally. Lesions were made using a stimulus generator (model SD9F; Grass, Quincy, MA, USA) and a linear stimulus isolator (model A395R; World Precision Instruments), which delivered 1.5 mA of d.c. current for 20–30 s. The sham control group ($n = 5$) experienced the same procedures except that current was not applied. Next, bipolar stainless steel hook electrodes (50 μm diameter; California Fine Wire, Grover Beach, CA, USA) were implanted bilaterally into the nuchal muscle to record electromyographic (EMG) activity. Given the absence of state-dependent neocortical electroencephalographic activity in rats before P11 (Gramsbergen, 1976; Mirmiran & Corner, 1982; Frank & Heller, 1997), we elected to use nuchal muscle activity as a measure of sleep and wakefulness. We have found that the nuchal EMG alone provides a highly reliable and reproducible measure of active sleep (AS), quiet sleep (QS) and wakefulness in neonates (Karlsson & Blumberg, 2002; Seelke & Blumberg, 2005; Seelke *et al*., 2005).

Procedure

After surgery, subjects recovered for 3 h inside a humidified incubator maintained at 34–35 °C. Subjects were then intubated and infused with warm commercial half-and-half (50% whole milk and 50% cream) using a tracheal cannula; the volume (mL) was 2–4% of body weight. Immediately after infusion, subjects were placed inside a double-walled glass testing chamber (height, 17.0 cm; i.d., 12.5 cm), through which temperature-controlled water was circulated. Air temperature inside the chamber was maintained at 35.25 °C, which is within the thermoneutral range for rats at the ages used here (Spiers & Adair, 1986). Humidified airflow through the chamber was maintained at 300 mL/min, and a microcamera was located above the chamber's Plexiglas lid to record subjects' behavior in synchrony with EMG data. Finally, a Faraday cage was placed around the chamber. Subjects were allowed 1 h to acclimate to the chamber, after which behavior and EMG data were recorded for 1 h. The rapid cyclicity of infant sleep allows for a sufficient number of representative sleep–wake transitions to be obtained within 1 h (Karlsson & Blumberg, 2002; Karlsson *et al*., 2004).

Because damage to the POA and BF is known to disinhibit heat production in both adults (Szymusiak, 1995) and infants (Blumberg *et al*., 1995), subjects' body temperatures were closely monitored following surgery. Temperature readings from the interscapular area as well as the lower back were obtained using a chromel–constantan thermocouple (Omega, Stamford, CT, USA) applied to the skin until a stable reading was obtained. These temperature measures were used to determine whether thermogenesis by brown adipose tissue (BAT) was disinhibited after the lesions (Blumberg *et al*., 1995). If, at the time of infusion 3 h after surgery, a subject's interscapular temperature exceeded the criterion of 38.5 °C, it was injected subcutaneously with propranolol (Aldrich, Milwaukee, WI, USA) to inhibit BAT heat production (dose, 20 mg/kg; volume, 1 μL/g body weight). Three of the five shams were given propranolol as a further control for the behavioral effects of this drug. Forty-five minutes after infusion and drug injection, temperatures were taken again to ensure that the subjects were normothermic at the beginning of the testing period. Finally, temperatures were measured at the end of the testing period to confirm thermal stability throughout the test.

All but one lesioned P9 subject exhibited a significant increase in body temperature and therefore propranolol was administered to block heat production. Thus, for both lesion and sham subjects, the range of interscapular temperatures was 36.7–38.3 °C at the beginning of the testing period and 36.9–38.5 °C at the end of the testing period. The POA + BF group also included one subject for which propranolol was ineffective, displaying an interscapular temperature of 39.5 °C at the end of the test; however, this subject did not display sleep and wake patterns that differed from those of its group. Finally, we found that propranolol administration had no effect on sham subjects' sleep and wake behavior in relation to untreated shams.

Data analysis

EMG signals were amplified (×10 000) and filtered (300–5000 Hz) using a differential amplifier (model 1700; A-M Systems, Carlsborg, WA, USA). EMG and video signals were recorded synchronously using a digital recording system (model DV8, Vetron, Rebersburg, PA, USA).

EMG signals were digitized at 2 kHz using a data acquisition system (BioPac Systems, Inc., Santa Barbara, CA, USA). Digitized signals were summed (when there were two usable EMG signals), integrated and full-wave rectified. The EMG signal was then dichotomized into bouts of sleep and wake as described previously (Karlsson *et al*., 2004). Briefly, the midpoint between average levels of atonia and high muscle tone was determined for each subject. Bouts of atonia (indicative of sleep) and high tone (indicative of wakefulness)

were defined as periods in which muscle tone was below or above, respectively, the midpoint value for at least 1 s.

Mean sleep and wake bout durations were determined for each subject by dividing its total amount of time spent in both states by its total number of sleep–wake cycles during the 1-h test period, with one cycle being defined as a sleep bout and its succeeding wake bout. This included 58–100 sleep–wake cycles for subjects in the POA group, 79–110 sleep–wake cycles for subjects in the BF group, 94–176 sleep–wake cycles for subjects in the POA + BF group and 63–127 sleep–wake cycles for subjects in the sham group. After mean sleep and wake bout durations were determined for each subject, mean sleep bout durations for all subjects within a group were then averaged, as were wake bout durations. In addition, the percentage of time in which subjects were awake or asleep was calculated. Analysis of variance (ANOVA) was used to test for group effects, and Fisher's PLSD was used for *post-hoc* tests. The value of alpha was set at 0.05. Means are presented with their standard errors (SEM).

In order to distinguish QS from AS, nuchal EMG records were analysed for phasic twitching activity as described previously (Seelke & Blumberg, 2005). Twitches of the nuchal muscle can be identified as high-amplitude spikes in the EMG record during periods that are dominated by atonia. For the present study, we defined a nuchal twitch as such a spike that was at least 3× the baseline during an atonia period as defined above. The first ten sleep bouts from each subject in each group were selected for analysis. The latency from the end of a wake period to the first twitch of a sleep period was defined as the period of QS, and the period between this first twitch and the onset of the next wake period was defined as the period of AS. The mean percentage of each sleep bout occupied by QS and AS within a group was then determined by combining the mean durations of QS and AS for the group, and then dividing the mean QS and AS durations by this sum. ANOVA was used to test for group effects, and Fisher's PLSD was used for *post-hoc* tests. Alpha was set at 0.05. Means are presented with their SEM. Subjects were excluded from further analysis if their lesions were misplaced or asymmetric ($n = 21$) or if their EMG records were unscorable ($n = 9$).

Histology

Immediately after testing, all subjects were given an overdose of sodium pentobarbital and perfused transcardially with phosphate-buffered saline followed by 3% formalin. Heads were post-fixed in a sucrose–formalin solution for at least 24 h, whereupon the brain was removed and post-fixed for at least an additional 24 h. Brains were then sliced in the coronal plane into 50-μm sections, which were mounted and stained with cresyl violet. The extent of each lesion was evaluated under a microscope and drawn onto an archival set of digitized photomicrographs using image software (Adobe Photoshop 5.5, Adobe, San Jose, CA, USA).

Precollicular transections in P2 rats

Surgery

Eleven P2 rats from seven litters were used (body weights, 6.5–9.4 g). Under isoflurane anesthesia, transections ($n = 6$) were made by first using a 23-gauge needle to drill an insertion point at approximately 3 mm caudal to lambda, and then manually inserting a blunted 25-gauge needle to the base of the brain and gently rotating the needle using a side-to-side motion (Karlsson *et al*., 2004). Sham controls ($n = 5$) experienced the same procedure except that the blunted needle was not inserted into the brain. Next, nuchal EMG electrodes were implanted.

Procedure

After surgery, subjects were allowed to recover, monitored, intubated, infused and tested as previously described. Again, skin temperatures were closely monitored. After precollicular transection or sham surgery in P2 rats, the range of interscapular temperatures was 35.8–37.8 °C at the beginning of the testing period and 36.1–37.6 °C at the end of the testing period. Thus, because no subjects in the transected (or sham) group exhibited body temperatures exceeding the 38.5 °C criterion, none was injected with propranolol.

Data analysis

EMG signals were dichotomized into sleep and wake bouts and analysed as described above. Mean sleep and wake bout durations were determined for each subject using its total number of sleep–wake cycles for the 1-h test period. This included 153–300 sleep–wake cycles in the transected group and 128–177 sleep–wake cycles in the sham group. Group differences in mean sleep and wake durations were tested using unpaired *t*-tests. Alpha was set at 0.05. Means are presented with their SEM.

Histology

Transected brains were prepared for histology using transcardial perfusion as described above. The rostrocaudal placement of the transection was then determined via gross visual inspection and drawn onto a photomicrograph of a P2 sagittal section.

Modafinil injections in P2 and P9 rats

Surgery

Ten P9 rats (body weights, 18.2–26.2 g) from five litters and nine P2 rats (body weights, 7.1–9.2 g) from five litters were used. Under isoflurane anesthesia, all subjects were implanted with nuchal EMG electrodes, as described above.

Procedure

After surgery, subjects were placed inside the previously described heated, humidified testing chamber, where they recovered and acclimated for 1 h. After the 1-h recovery and acclimation period, 30 min of synchronous EMG and behavioral baseline data were recorded. Following this baseline period, subjects in the modafinil group received intraperitoneal injections of 100 mg/kg modafinil (lot no. PA 003; Cephalon, Inc., West Chester, PA, USA) suspended in a solution of 0.25% methylcellulose (MP Biomedicals, LLC, Aurora, OH, USA) in 0.9% sterile saline. It has previously been demonstrated in adults rats and mice that intraperitoneal injection of a suspension of modafinil in methylcellulose and saline at a dose of 75–150 mg/kg promotes wakefulness (Scammell *et al*., 2000; Willie *et al*., 2005). Subjects in the control group received an equivalent amount of vehicle only. After injection of either modafinil or vehicle, EMG and behavioral data were recorded for 1 h. In pilot studies with infants, it was observed that modafinil injections had no effect on body temperature. Nonetheless, interscapular temperatures were recorded at the conclusion of each experiment to ensure normothermia during the test.

Data analysis

EMG signals were dichotomized into sleep and wake bouts and analysed as described above. The 30-min baseline recording period was compared with the first and second 30-min periods after injection.

Mean sleep and wake bout durations for each subject were determined from the total number of sleep–wake cycles completed during each recording period (the number of cycles ranged from four to 66 at P9 and from 38 to 110 at P2). Repeated-measures ANOVA was used to test for significant effects of modafinil on mean sleep and wake bout durations at each age. For *post-hoc* tests, paired *t*-tests were used to compare changes in bout durations from baseline. Alpha was set at 0.05 and the Bonferroni correction procedure was used to correct for multiple comparisons. In one case, the data for a P9 subject in the modafinil group were excluded because this subject's mean high-tone duration exceeded the group mean ± 1.96 standard deviations. Means are presented with their SEM.

Neurophysiology in P9 rats

Surgery

Nine P9 rats from nine litters were used (body weights, 17.8–23.1 g). Under isoflurane anesthesia, the subjects' fragile skulls were bleached, dried and coated with Vetbond (3M, St. Paul, MN, USA) to add strength. Next, a custom-built, T-shaped, stainless steel head-plant, designed to attach to the earbar and nosebar holders of a stereotaxic apparatus, was attached to the skull over the pretreated area using cyanoacrylate adhesive gel (Karlsson *et al*., 2005). Nuchal EMG electrodes were implanted as described above. After securing the head-plant and leveling the skull, a small hole was drilled over the intended recording site for insertion of the electrode. Finally, to inhibit movement and to calm the subject, it was wrapped in gauze (Corner & Kwee, 1976).

Procedure

Recordings were performed in a stereotaxic apparatus with body and brain temperatures maintained at approximately 37 °C. In contrast to adults (Lee *et al*., 2004), infant rats do not require extensive habituation to exhibit sleep–wake cyclicity when head-fixed in the recording apparatus. Thus, within 2–3 h after surgery, pups had begun exhibiting oscillations in muscle tone as well as myoclonic twitches against a background of nuchal atonia. When such sleep–wake cyclicity was observed, a stainless steel 8-trode (ALA Science, Westbury, New York, NY, USA), connected to a unity gain headstage and digital amplifier (Tucker-Davis Technologies, Alachua, FL, USA), was lowered into the brain while neurophysiological activity was monitored using an oscilloscope and audio analyser (FHC, Bowdoinham, ME, USA). The 8-trode consisted of eight individual recording sites distributed around the tip (500–800 kΩ per electrode), with the entire electrode having a diameter of approximately 150 μm. The signals were amplified (10 k) and filtered (500–5000 Hz band-pass) before being sampled at 12.5 kHz. When stable units were observed and at least one of these units appeared to exhibit state-dependent activity, the electrode was left in place for 5–10 min before data collection began. Neurophysiological and EMG data were recorded synchronously for 10–15 min to hard disk for off-line analysis. At the end of the experiment, the most ventral and most dorsal recording sites were marked by passing a 50-μA anodal current through the eight closely spaced electrodes for 3 s, thereby producing a single small lesion at both locations.

Data analysis

Two or four of the eight continuously recorded channels containing heterogeneous unit activity were selected for off-line analysis. Using Spike2 software (Cambridge Electronic Design, Ltd, Cambridge, UK), a threshold was set for each of the selected channels to extract spike data with a signal-to-noise ratio of at least 2 : 1. Using the multichannel data, principal components analysis was then used for spike sorting (Abeles & Goldstein, 1977; Lewicki, 1998). The sorted units were assigned to groups using graphical cluster cutting. To remove artificial clusters, spike waveforms were inspected and autocorrelations were constructed for each cluster. A cluster was judged to contain a single unit only if the autocorrelation analysis indicated a refractory period of at least 2 ms.

Two types of analyses were performed on the sorted units using procedures similar to those described previously (Karlsson *et al*., 2005). The first analysis was carried out to classify each of the recorded neurons as sleep-on, wake-on or sleep/wake-indifferent. Periods of sleep and wakefulness were identified from the EMG record as described above, and the firing rates of individual sorted units were compared with the behavioral state of the subject across the total number of sleep–wake cycles present during the recording period. This included 9–36 pairs of sleep and wake periods for subjects in the POA group ($n = 2$) and 18–58 pairs of sleep and wake periods for subjects in the BF group ($n = 4$). State-related differences in mean discharge rates were tested using the Wilcoxon matched-pairs signed-ranks test; alpha was set at 0.05. Neurons that significantly increased their firing rates during sleep or wake periods were classified as sleep-on or wake-on, respectively. Neurons with firing rates that did not differ between sleep and wake bouts were classified as sleep/wake-indifferent.

The second analysis was performed on sleep-on and wake-on neurons to determine further whether discharge rates differed between sleep bouts that did or did not contain the phasic myoclonic twitching indicative of AS (Karlsson *et al*., 2005). Discharge rates during the first ten 4-s segments of atonia with no nuchal EMG spikes (indicative of sleep without phasic processes, i.e. QS) and discharge rates during the first ten 4-s segments of atonia with more than four nuchal EMG spikes (indicative of sleep with phasic processes, i.e. AS) were compared using the Mann–Whitney *U*-test; alpha was set at 0.05. (At two POA recording sites and at one BF recording site, only 7–9 bouts of atonia were available that could be classified in this way.) Neurons that showed a significantly elevated rate of firing during AS or QS were classified as AS-on or QS-on, respectively. Neurons that showed no preferential increase in firing during either AS or QS were classified as AS/QS-indifferent. Within a single sleep period, no more than one bout of QS and AS was considered for analysis. Means are presented with their SEM. Three subjects were excluded from further analysis owing to unclear marking lesions.

Histology

Brains were prepared for histological analysis using transcardial perfusion as described above. After fixation, brains were sliced into 50-μm sections with a sliding microtome, and these were then stained with cresyl violet or nuclear red. The locations of the marking lesions were determined by examining serial sections.

Results

POA and BF lesions differentially affect sleep and wakefulness

The extent of the neural damage for the five rats with bilateral POA lesions is shown in the left panel of Fig. 1A. The lesions are well localized to the POA, with each lesion ablating the ventral area designated as the VLPO in infants and adults (Chamberlin *et al*., 2003). Even the smallest lesions were large enough to destroy the VLPO at this coronal level as well as throughout the majority of its

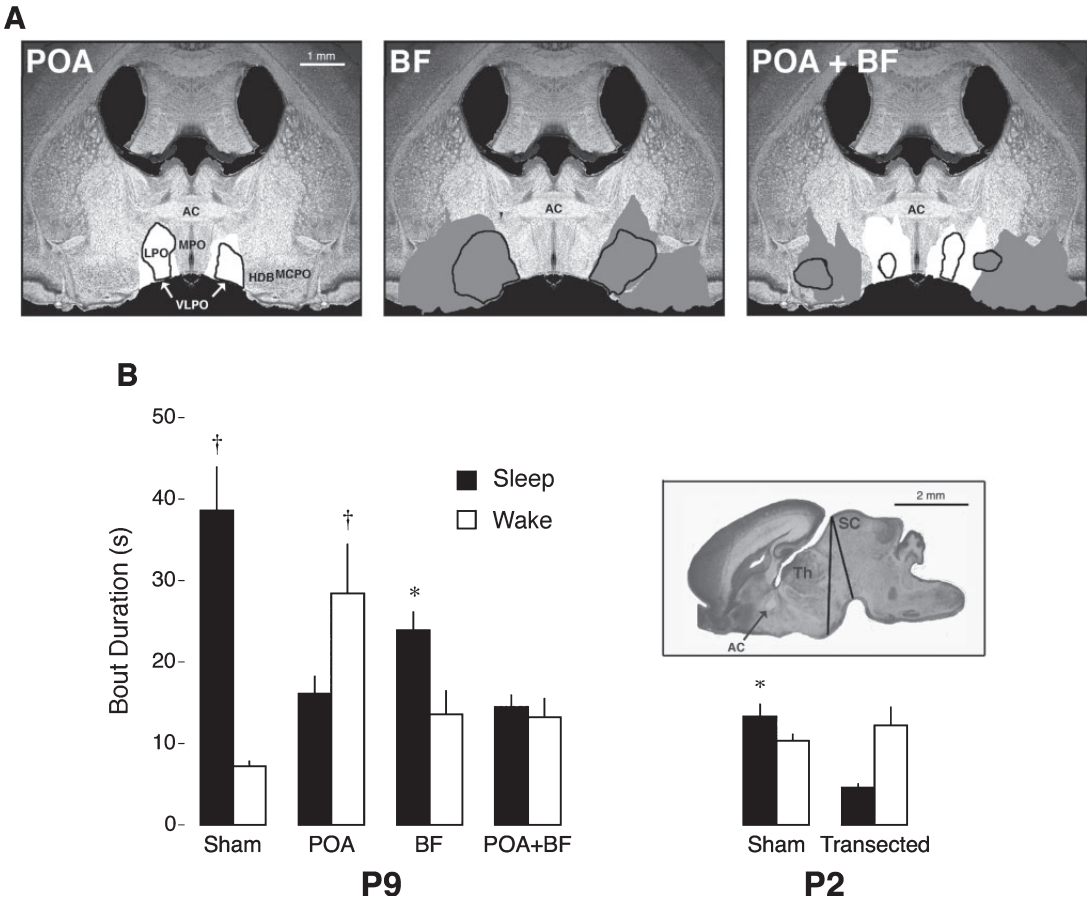

FIG. 1. Effects of lesions and transections on sleep and wake bout durations in infant rats. (A) Reconstructions of the lesions in the preoptic area (POA) (white), basal forebrain (BF) (gray) and POA + BF in P9 rats. White and gray areas indicate the cumulative lesioned areas across all subjects in each group; the smaller areas outlined in black indicate the smallest lesion within each group. (B) Left: mean sleep and wake bout durations for the sham and lesion groups. †Significantly greater than all other groups. *Significantly greater than the POA + BF group. Right: mean sleep and wake bout durations for the P2 subjects with precollicular transections or sham transections. *Significantly greater than transected group. Inset: mid-sagittal section from a P2 rat brain, with the rostrocaudal range of the transections depicted. $n = 5$–6 subjects per group. Mean + SEM. AC, anterior commissure; HDB, horizontal limb of the diagonal band; LPO, lateral preoptic area; MCPO, magnocellular preoptic area; MPO, medial preoptic area; SC, superior colliculus; Th, thalamus; VLPO, ventrolateral preoptic area.

rostrocaudal extent, as defined previously (Sherin *et al*., 1998). The lesions generally did not extend beyond the rostrocaudal borders of the VLPO [and therefore did not encroach upon the suprachiasmatic nucleus (SCN)], but did include regions of the more dorsally located LPO as well as lateral regions of the MPO. It should be stressed, however, that the POA lesions encroached only negligibly upon the BF.

The extent of the neural damage for the five rats with bilateral BF lesions is shown in the middle panel of Fig. 1A. After analysing the sleep and wake data from this lesion group, we found no basis for distinguishing between subjects with more medial vs. more lateral lesions. BF lesions exhibited a similar rostrocaudal extent as POA lesions and did not extend medially beyond the horizontal limb of the diagonal band, indicating that these lesions produced minimal damage within the POA. Some rats with more laterally placed BF lesions sustained damage to portions of the piriform cortex and anterior amygdaloid regions; these are regions, however, that have not been implicated in the regulation of sleep and wakefulness.

The extent of the neural damage for the five rats with bilateral POA + BF lesions is shown in the right panel of Fig. 1A. Figure 1A presents a composite of all lesions for subjects within this group (it should be noted that the four individual lesions for each subject never overlapped). The spatial profiles of these lesions were similar to those

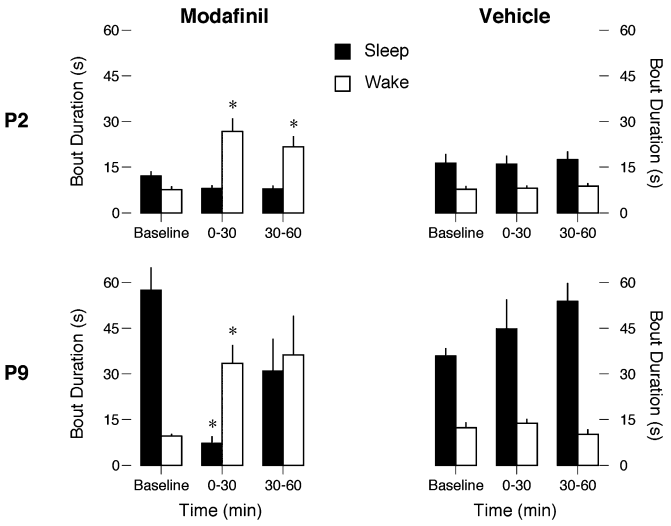

FIG. 2. Effects of modafinil administration (100 mg/kg, i.p.) on mean sleep and wake bout durations in infant rats at P2 and P9. For each subject, nuchal muscle tone was recorded for 30 min before injection of modafinil or vehicle (Baseline) and for two 30-min periods after injection. $n = 4$–5 subjects per group. Mean + SEM. *Significantly greater than baseline.

described above for the POA and BF lesion groups. As was the case for the BF lesion group, some subjects in the POA + BF group with more laterally placed BF lesions sustained damage to portions of the piriform cortex and anterior amygdaloid area. The POA + BF group also included one subject with slight unilateral encroachment onto the SCN.

Whereas mean durations of sleep bouts differed between experimental groups, no significant differences were found in the percentage of each sleep bout that was occupied by AS or QS ($F_{3,16} = 0.8$), which comprised 66.0 ± 4.9 and 34.0 ± 4.9% of each bout, respectively. Regardless of the type of lesion produced, decreases in sleep bout durations were characterized by proportionate decreases in both AS and QS.

There was a significant effect of group on mean sleep bout durations ($F_{3,16} = 12.3$, $P < 0.001$) and mean wake bout durations ($F_{3,16} = 6.5$, $P < 0.005$). As shown in Fig. 1B, the POA + BF lesion group exhibited a significant decrease in sleep bout durations, but no change in wake bout durations, in relation to the sham group. Subjects with separate lesions of only the POA or BF exhibited intermediate and largely opposite patterns of sleep and wakefulness. First, the POA lesion group exhibited a reduction in sleep durations similar to that of the POA + BF group, but wake durations were significantly elevated in relation to all other groups. Second, the BF group also exhibited a reduction in sleep durations but without an increase in wake durations. The result was that the POA and BF lesions produced subjects with sleep cycles predominated by wakefulness and sleep, respectively.

Consideration of the total percentage of time that subjects spent asleep helps to illustrate further the effects of these lesions. In the sham group, the mean percentage of the test period spent asleep was 82.8 ± 3.4%, whereas the value for the POA + BF group was 53.5 ± 5.0%. The values for the POA and BF groups straddled the 50% mark with values of 38.5 ± 7.7 and 64.3 ± 6.2%, respectively. The effect of group on the percentage of time that subjects spent asleep was significant ($F_{3,16} = 10.3$, $P < 0.001$).

Precollicular transections in P2 rats decrease mean sleep bout durations

Gross inspection of the transected brains indicated that most were completely separated; for the remainder, only small portions of the dorsal or lateral cerebral cortex remained intact. The inset in Fig. 1B presents a mid-sagittal section from a P2 rat and illustrates the rostrocaudal range of the transections.

As shown in Fig. 1B, precollicular transections produced a significant reduction in mean sleep bout durations ($t_9 = 7.1$, $P < 0.0001$) but did not affect mean wake bout durations ($t_9 = 0.8$, NS). In addition, transected subjects spent an average of 30.2 ± 5.4% of the test period asleep, which is significantly less than the 57.9 ± 4.0% exhibited by shams ($t_9 = 27.7$, $P < 0.005$).

Effect of modafinil administration on sleep and wakefulness at P2 and P9

Administration of modafinil (100 mg/kg) produced marked increases in wake behavior in subjects at both ages. Nonetheless, subjects did cycle between sleep and wakefulness throughout each of the two 30-min post-injection periods, thus allowing us to analyse mean sleep and wake bout durations as described above for lesioned subjects. As shown in Fig. 2, modafinil administration at P9 decreased mean sleep bout duration ($F_{1,8} = 7.6$, $P < 0.05$) and increased mean wake bout

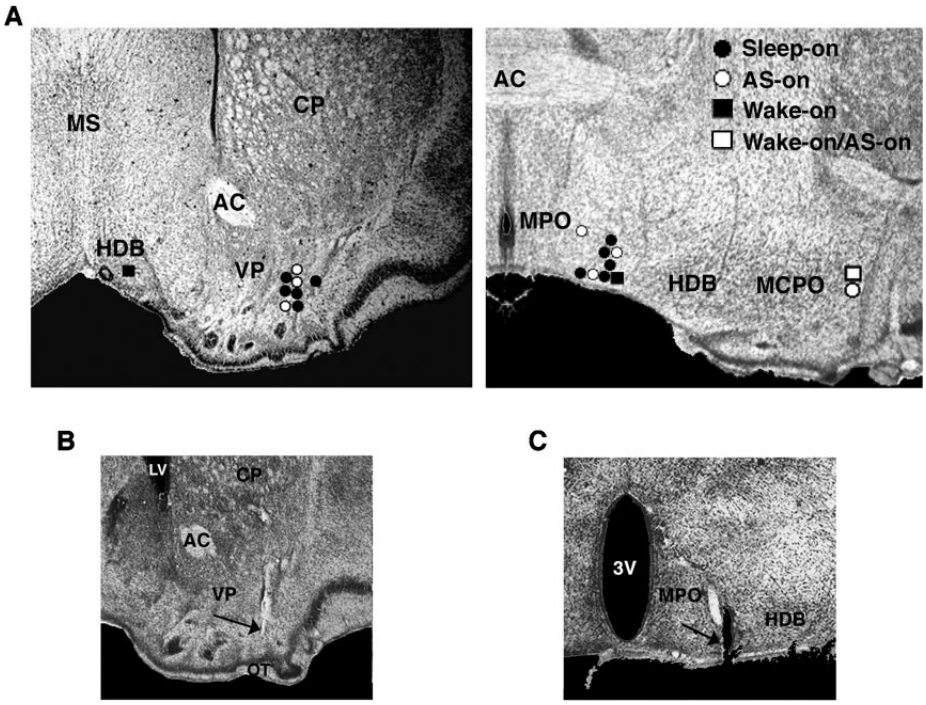

FIG. 3. Locations of state-dependent neurons within the preoptic area (POA) and basal forebrain (BF). (A) Recording sites of state-dependent neurons reconstructed on coronal sections of the POA and BF of a P9 rat. The section on the left is approximately 300 μm rostral to the section on the right. Symbols are shown for four classes of state-dependent neurons. (B) Photomicrograph depicting the location of one recording site within the BF. Black arrow indicates the location of the electrode track, along which recordings were taken. (C) Photomicrograph depicting the location of one recording site within the POA. Black arrow indicates the location of the electrode track, along which recordings were taken. 3V, third ventricle; AC, anterior commissure; CP, caudate putamen; HDB, horizontal limb of the diagonal band; LV, lateral ventricle; MCPO, magnocellular preoptic area; MPO, medial preoptic area; MS, medial septum; OT, olfactory tubercle; VP, ventral pallidum.

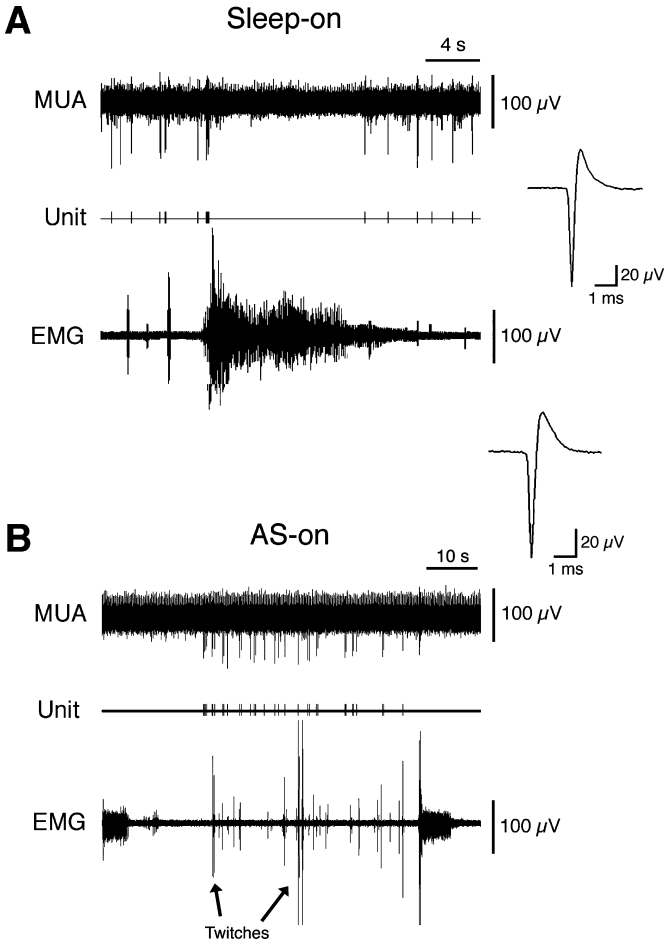

FIG. 4. State-dependent neural activity within the preoptic area of hypothalamus. (A) Representative sleep-on neuron. Upper trace: multi-unit activity (MUA). Middle trace: activity of one isolated unit derived from the MUA; its average waveform is shown at far right. Lower trace: concurrently recorded nuchal EMG. (B) Representative AS-on neuron. Upper trace: MUA. Middle trace: activity of one isolated unit derived from the MUA; its average waveform is shown at far right. Lower trace: concurrently recorded nuchal EMG. Arrows indicate myoclonic twitches produced against a background of muscle atonia, indicative of AS.

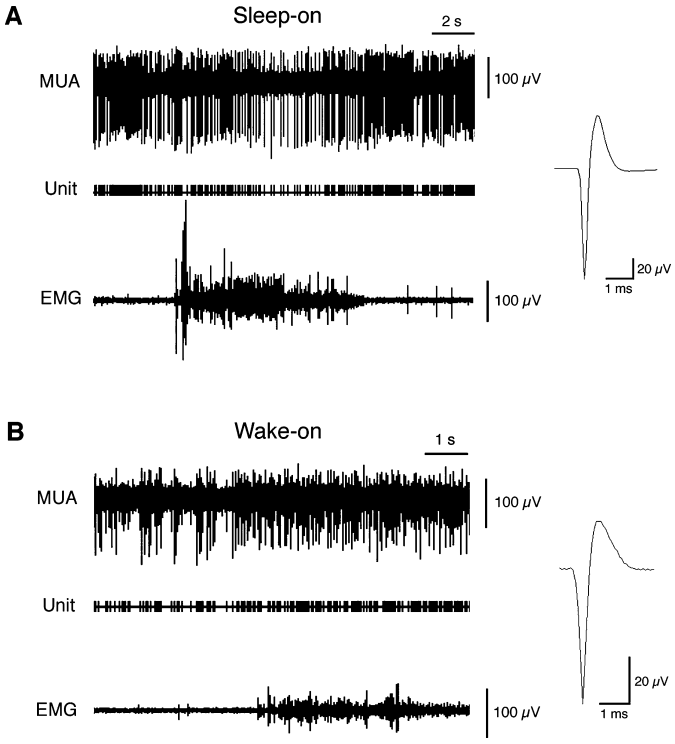

FIG. 5. State-dependent neural activity within the basal forebrain. (A) Representative sleep-on neuron. Upper trace: multi-unit activity (MUA). Middle trace: activity of one isolated unit derived from the MUA; its average waveform is shown at far right. Lower trace: concurrently recorded nuchal EMG. (B) Representative wake-on neuron. Upper trace: MUA. Middle trace: activity of one isolated unit derived from the MUA; its average waveform is shown at far right. Lower trace: concurrently recorded nuchal EMG.

duration ($F_{1,8} = 23.7$, $P < 0.005$) in relation to controls. By contrast, at P2, modafinil produced only a significant increase in mean wake bout duration ($F_{1,7} = 7.5$, $P < 0.05$).

At P9 there was also a significant group–time interaction for mean sleep bout durations ($F_{2,16} = 3.9$, $P < 0.05$) and mean wake bout durations ($F_{2,16} = 10.4$, $P < 0.005$), in addition to a significant effect of time on mean wake bout durations ($F_{2,16} = 11.8$, $P < 0.001$). At P2 there was again a significant group–time interaction for mean sleep bout durations ($F_{2,14} = 14.6$, $P < 0.01$) and mean wake bout durations ($F_{2,14} = 6.1$, $P < 0.05$), as well as a significant effect of time on mean sleep bout durations ($F_{2,14} = 7.3$, $P < 0.01$) and mean wake bout durations ($F_{2,14} = 5.6$, $P < 0.05$).

The infant POA and BF contain neurons that exhibit state-dependent activity

In total, 41 neurons were recorded from six P9 rats (1–15 neurons per rat; 1–4 neurons per recording site), and each of these neurons was classified based upon the specific relationship of its activity to the components of sleep and wakefulness. Figure 3A presents coronal sections with composite representations of the anatomical locations at which different types of sleep- and wake-related neurons were found. Figure 3B and C are photomicrographs of examples of recording sites within the BF and POA, respectively.

A total of 20 neurons were recorded from the POA (2 rats; 6–14 neurons per rat; 3–4 neurons per recording site), 15 of which showed state-dependent firing patterns (Fig. 4). Twenty-one neurons were recorded from the BF (4 rats; 1–15 neurons per rat; 1–3 neurons per recording site), 14 of which showed state dependency (Fig. 5). The firing rates of the state-dependent POA and BF neurons are shown in Table 1.

Discussion

Given that chronic POA lesions produce an approximately 50% reduction in sleep bout durations (Lu *et al*., 2000), it could reasonably be inferred that the similar results produced by acute precollicular transections in infant rats (Karlsson *et al*., 2004) occur because they disconnect the POA from more caudal projection sites. Indeed, as shown here, lesioning the infant POA did result in an approximately 50% reduction in sleep bout durations. Unexpectedly, however, these lesions also produced a quadrupling of wake bout durations. This last finding implies the existence of a caudally projecting, wake-promoting area within the forebrain that becomes disinhibited directly and/or indirectly after lesioning of the POA. If true, then the rapid sleep–wake cycles produced by the precollicular transections of Karlsson *et al*. (2004) likely resulted from the simultaneous elimination of

TABLE 1. Number and firing rates of neurons recorded from the preoptic area (POA) and basal forebrain (BF)

		Firing rate (Hz)			
	n	Sleep	Wakefulness	Active sleep (AS)	Quiet sleep (QS)
POA					
Sleep-on neurons	14	0.81 ± 0.11	0.41 ± 0.09	–	–
AS-on neurons	4	–	–	1.40 ± 0.24	0.49 ± 0.20
Wake-on neurons	1	0.57	1.45	–	–
State-indifferent neurons	5	0.70 ± 0.21	0.71 ± 0.29	–	–
BF					
Sleep-on neurons	11	8.01 ± 1.78	5.52 ± 1.50	–	–
AS-on neurons	4	–	–	10.44 ± 3.30	6.67 ± 3.32
Wake-on neurons	3	10.84 ± 4.51	12.87 ± 4.48	–	–
Wake-on/AS-on neurons	1	–	–	5.42	1.40
State-indifferent neurons	7	3.08 ± 0.96	3.00 ± 1.08	–	–

Data are presented as means ± SEM. State-dependent neurons within the POA and BF are classified as sleep-on, wake-on, or state-indifferent, and neurons are further subclassified as AS-on or wake-on/AS-on neurons.

descending influences from the sleep-promoting POA as well as the wake-promoting region disinhibited by POA lesions. Based on the present results, it appears that the BF may be this wake-promoting region.

In contrast to the differential effects of lesioning the POA or BF alone, the effect of lesioning the POA + BF was similar to that of Karlsson *et al*.'s (2004) precollicular transections. POA + BF-lesioned subjects displayed the significant decrease in sleep bout durations typical of POA-lesioned subjects, but without the corresponding significant increase in wake bout durations. Thus, as Fig. 1B indicates, the POA + BF-lesioned subjects exhibit sleep bout durations typical of POA-lesioned subjects and wake bout durations typical of BF-lesioned subjects.

Because distinct non-REM- (NREM) and REM-active areas within subregions of the adult POA (Szymusiak *et al*., 1998; Lu *et al*., 2002) and BF (Szymusiak & McGinty, 1986) have been identified, we sought to determine whether our lesions were preferentially depriving subjects of QS or AS. However, we found that although lesioned subjects exhibited shortened sleep bouts, the percentage of each sleep bout occupied by QS or AS did not differ between sham and lesioned subjects. Thus, none of our lesions differentially affected QS or AS. It was not possible, however, to determine histologically the extent of damage to NREM- and REM-active regions within the POA and BF. Importantly, and in contrast to lesions within the medulla and mesopontine regions (Karlsson & Blumberg, 2005; Karlsson *et al*., 2005), none of the lesions in this study disrupted the tight linkage between muscle atonia and myoclonic twitching.

While Lu *et al*. (2000) and others have used ibotenic acid to produce POA lesions in adults, the use of chemical lesions in infants presents unique challenges. For example, although we have found that quisqualic acid can be used to produce rapid lesions in infant rats within some medullary and mesopontine nuclei (Karlsson & Blumberg, 2005; Karlsson *et al*., 2005), our attempts to produce chemical lesions in the POA of infants were unsuccessful. Therefore, we chose to use electrolytic lesions in this study. The well-known pitfalls of electrolytic lesions (i.e. destruction of fibers of passage) are mitigated somewhat by the fact that Karlsson *et al*. (2004) found that sleep–wake cycles were unaffected by transections that were rostral to the POA, thus suggesting that the effects of the electrolytic lesions reported here were not due to destruction of axons passing through the lesioned areas from more rostral structures.

Karlsson *et al*.'s (2004) finding that precollicular transections in P8 rats resulted in sleep–wake cycles characteristic of P2 rats might have been interpreted as evidence that P2 rats do not yet utilize forebrain structures in the generation and/or maintenance of sleep and wake states. To address this issue, we performed analogous transections in P2 rats and, interestingly, we found that, just as in P9 rats, this manipulation decreased sleep bout durations without affecting wake bout durations. This finding suggests that forebrain structures already modulate sleep–wake activity at P2, perhaps a surprising finding in light of the claim that even brainstem neural mechanisms are probably not involved in sleep–wake control at this age (Frank & Heller, 2003). Moreover, the finding that modafinil had a less potent sleep-inhibiting effect at P2 seems to suggest that the influence of the POA on more caudal regions increases during the first postnatal week, perhaps

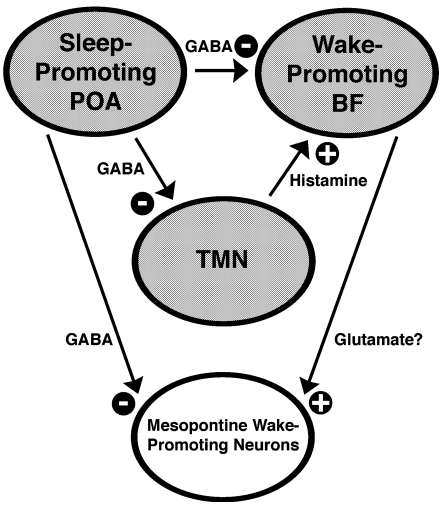

FIG. 6. Proposed model to explain why lesions of the preoptic area (POA) reduce sleep bout durations but lengthen wake bout durations. Arrows depict known excitatory (+) and inhibitory (–) connections between the POA and the wake-promoting basal forebrain (BF), tuberomammillary nucleus (TMN), and mesopontine wake-promoting neurons (e.g. in locus coeruleus and dorsal raphe); reciprocal connections between these regions are not shown. According to this model, POA lesions reduce sleep bout durations by destroying sleep-promoting neurons in that region. The lengthening of wake bout durations arise from (1) the removal of direct GABAergic inhibition of the BF and (2) the removal of GABAergic inhibition of the TMN, thereby producing increased histaminergic excitatory input to the BF. In this way, wake-promoting mesopontine neurons are activated as a result of increased excitation from the BF and decreased inhibition from the POA.

facilitating the developmental increase in sleep bout duration. It is important to note, however, that although one *in vitro* study has hypothesized that modafinil exerts its effects via the POA (Gallopin *et al*., 2004), its exact mechanism of action is presently unknown (Saper & Scammell, 2004). In addition, the mechanism by which the POA and other structures come to exert increased modulatory control over more caudal neural circuits across development remains unknown at this time.

In the current study, we document for the first time the existence of state-dependent neural activity within the infant hypothalamus. Our finding that the majority of state-dependent POA neurons were preferentially active during sleep (i.e. sleep-on) is consistent with the results of other electrophysiological studies in adult rats (Koyama & Hayaishi, 1994; Szymusiak *et al*., 1998), as well as several studies quantifying c-Fos expression in the adult POA (Sherin *et al*., 1996; Gong *et al*., 2000). Although the firing rates of these neurons were significantly higher during sleep than during wakefulness, we were surprised to find that these rates were much lower than those previously reported in adults (Koyama & Hayaishi, 1994; Szymusiak *et al*., 1998). The fact that the majority of state-dependent neurons recorded from the infant BF were sleep-on was also surprising, because most state-dependent BF neurons in adults have previously been reported to be wake-on/REM-on (Szymusiak & McGinty, 1986, 1989).

It is as yet unclear why POA neurons would discharge at lower rates in infants than in adults, and also why the infant BF appears to contain such a large population of sleep-on neurons. These discrepancies may reflect our relatively small sample of neurons. However, it must be remembered that our goal here was simply to demonstrate the existence of state-dependent neurons in the infant forebrain, not to provide a quantitative estimate of the subpopulations contained therein. For this purpose, our sample is sufficiently large. The fact that lesions of the POA and BF altered sleep–wake activity suggests that the neurons in these areas play a causal role in the modulation of sleep–wake activity at this age. Of course, additional research is needed to identify the neurochemical phenotypes of these neurons, as well as the proportions of neurons preferentially active during sleep and wakefulness across the early postnatal period.

We propose a working model to account for the effects of the POA, BF and POA + BF lesions reported here within the context of known neural circuitry (see Fig. 6). Although the POA sends inhibitory projections to many wake-promoting nuclei, a particularly strong projection exists from the POA to the TMN (Ericson *et al*., 1991; Sherin *et al*., 1998; Steininger *et al*., 2001), where POA neurons have been shown to inhibit histaminergic neurons *in vitro* (Yang & Hatton, 1997). Although the TMN sends excitatory histaminergic efferents to many areas of the brain, it projects most strongly to more rostral areas within the forebrain, including the wake-promoting BF (Staines *et al*., 1987a,b). TMN modulation of forebrain activity may also be mediated through GABA, which is co-localized with histamine in TMN neurons (Brown *et al*., 2001).

When histamine is applied locally into the cholinergic BF of adult rats, it produces increased wakefulness and decreased NREM sleep (Ramesh *et al*., 2004), resulting in a behavioral effect similar to that seen with our POA lesions. Hence, the wake-promoting effect of the POA lesion may be mediated by disinhibition of the TMN's histaminergic excitation of the wake-active BF, in addition to the simultaneous abatement of direct POA GABAergic inhibition of the wake-active BF. This scenario is supported by *in vitro* data indicating excitation of BF cholinergic and putative glutamatergic neurons by histamine (Khateb *et al*., 1995; Fort *et al*., 1998). Additionally, BF cholinergic neurons are inhibited by GABA *in vitro* (Khateb *et al*., 1998). As is the case for the TMN, there is also evidence that the POA projects to regions of the posterior hypothalamus where orexinergic neurons are found (Sherin *et al*., 1998), which in turn project to the BF (Peyron *et al*., 1998; Espana *et al*., 2005).

In summary, both POA and BF lesions reduced sleep bout durations, suggesting that these areas contribute to sleep promotion in infant rats. The presence of sleep- and AS-on neurons in both areas, as shown here, is consistent with this suggestion. However, the parallels between the functions of these two areas end there, as POA lesions also produced an unexpected increase in wake bout durations that was prevented by combined lesions of both areas. Figure 6 provides one possible explanation for this asymmetric relationship between POA and BF functioning, showing that although the removal of the POA leads to reduced sleep bout durations, it seems to be the sparing of the BF that leads to increased wake bout durations. Our results indicate that the effects of modafinil on sleep and wakefulness are very similar to those of POA lesions and, moreover, its differential effects on sleep and wakefulness at P2 and P9 may reflect the increasing functional importance of the POA across development. The present results therefore suggest that the POA and BF play opposing roles in the descending modulation of sleep–wake cyclicity, and that the magnitude of this descending influence increases during the first postnatal week.

Acknowledgements

This sudy was supported by National Institute of Mental Health grants MH50701 and MH66424 (M.S.B). Modafinil was kindly provided by Cephalon, Inc. We thank Cynthia Shaw, Scott Robinson, Adele Seelke, Jessica Middlemis-Brown and Eric Johnson for their assistance.

Abbreviations

AS, active sleep; BAT, brown adipose tissue; BF, basal forebrain; EMG, electromyographic; LPO, lateral preoptic area; MPO, medial preoptic area; NREM, non-rapid eye movement; P, postnatal day; POA, preoptic area; QS, quiet sleep; REM, rapid eye movement; SCN, suprachiasmatic nucleus; TMN, tuberomammillary nucleus; VLPO, ventrolateral preoptic area; VP, ventral pallidum.

References

Abeles, M. & Goldstein, M.H. (1977) Multispike train analysis. *Proc. IEEE*, **65**, 762–773.

Blumberg, M.S., Schalk, S.L. & Sokoloff, G. (1995) Pontine and basal forebrain transections disinhibit brown fat thermogenesis in neonatal rats. *Brain Res.*, **699**, 214–220.

Brown, R.E., Stevens, D.R. & Haas, H.L. (2001) The physiology of brain histamine. *Prog. Neurobiol.*, **63**, 637–672.

Chamberlin, N.L., Arrigoni, E., Chou, T.C., Scammell, T.E., Greene, R.W. & Saper, C.B. (2003) Effects of adenosine on gabaergic synaptic inputs to identified ventrolateral preoptic neurons. *Neuroscience*, **119**, 913–918.

Chou, T.C., Bjorkum, A.A., Gaus, S.E., Lu, J., Scammell, T.E. & Saper, C.B. (2002) Afferents to the ventrolateral preoptic nucleus. *J. Neurosci.*, **22**, 977–990.

Corner, M.A. & Kwee, P. (1976) Cyclic EEG and motility patterns during sleep in restrained infant rats. *Electroencephalogr. Clin. Neurophysiol.*, **41**, 64–72.

Ericson, H., Blomqvist, A. & Kohler, C. (1991) Origin of neuronal inputs to the region of the tuberomammillary nucleus of the rat brain. *J. Comp. Neurol.*, **311**, 45–64.

Espana, R.A., Reis, K.M., Valentino, R.J. & Berridge, C.W. (2005) Organization of hypocretin/orexin efferents to locus coeruleus and basal forebrain arousal-related structures. *J. Comp. Neurol.*, **484**, 160–178.

Fort, P., Khateb, A., Serafin, M., Muhlethaler, M. & Jones, B.E. (1998) Pharmacological characterization and differentiation of non-cholinergic nucleus basalis neurons in vitro. *Neuroreport*, **9**, 61–65.

Frank, M.G. & Heller, H.C. (1997) Development of REM and slow wave sleep in the rat. *Am. J. Physiol.*, **272**, R1792–R1799.

Frank, M.G. & Heller, H.C. (2003) The ontogeny of mammalian sleep: a reappraisal of alternative hypotheses. *J. Sleep Res.*, **12**, 25–34.
Gallopin, T., Fort, P., Eggermann, E., Caull, B., Luppi, P.H., Rossier, J., Audinat, E., Mühlethaler, M. & Serafin, M. (2000) Identification of sleep-promoting neurons in vitro. *Nature*, **404**, 992–995.
Gallopin, T., Luppi, P.H., Rambert, F.A., Frydman, A. & Fort, P. (2004) Effect of the wake-promoting agent modafinil on sleep-promoting neurons from the ventrolateral preoptic nucleus: an in vitro pharmacologic study. *Sleep*, **27**, 19–25.
Gong, H., Szymusiak, R., King, J., Steininger, T. & McGinty, D. (2000) Sleep-related c-Fos protein expression in the preoptic hypothalamus: effects of ambient warming. *Am. J. Physiol.*, **279**, R2079–R2088.
Gramsbergen, A. (1976) The development of the EEG in the rat. *Dev. Psychobiol.*, **9**, 501–515.
Gramsbergen, A., Schwartze, P. & Prechtl, H.F.R. (1970) The postnatal development of behavioral states in the rat. *Dev. Psychobiol.*, **3**, 267–280.
Grove, E.A. (1988) Efferent connections of the substantia innominata in the rat. *J. Compar. Neurol.*, **277**, 347–364.
Jones, B.E. (2003) Arousal systems. *Front. Biosci.*, **8**, 438–451.
Karlsson, K.Æ. & Blumberg, M.S. (2002) The union of the state: myoclonic twitching is coupled with nuchal muscle atonia in infant rats. *Behav. Neurosci.*, **116**, 912–917.
Karlsson, K.Æ. & Blumberg, M.S. (2005) Active medullary control of atonia in week-old rats. *Neuroscience*, **130**, 275–283.
Karlsson, K.Æ., Gall, A.J., Mohns, E.J., Seelke, A.M.H. & Blumberg, M.S. (2005) The neural substrates of infant sleep in rats. *PLoS Biol.*, **3**, 891–901.
Karlsson, K.Æ., Kreider, J.C. & Blumberg, M.S. (2004) Hypothalamic contribution to sleep–wake cycle development. *Neuroscience*, **123**, 575–582.
Khateb, A., Fort, P., Pegna, A., Jones, B.E. & Muhlethaler, M. (1995) Cholinergic nucleus basalis neurons are excited by histamine in vitro. *Neuroscience*, **69**, 495–506.
Khateb, A., Fort, P., Williams, S., Serafin, M., Muhlethaler, M. & Jones, B.E. (1998) GABAergic input to cholinergic nucleus basalis neurons. *Neuroscience*, **86**, 937–947.
Kleitman, N. & Engelmann, T.G. (1953) Sleep characteristics of infants. *J. Appl. Physiol.*, **6**, 269–282.
Koyama, Y. & Hayaishi, O. (1994) Firing of neurons in the preoptic/anterior hypothalamic areas in rat: its possible involvement in slow wave sleep and paradoxical sleep. *Neurosci. Res.*, **19**, 31–38.
Lee, M.G., Manns, I.D., Alonso, A. & Jones, B.E. (2004) Sleep–wake related discharge properties of basal forebrain neurons recorded with micropipettes in head-fixed rats. *J. Neurophysiol.*, **92**, 1182–1198.
Lewicki, M.S. (1998) A review of methods for spike sorting: the detection and classification of neural action potentials. *Network: Computation Neural Systems*, **9**, R53–R78.
Lu, J., Bjorkum, A.A., Xu, M., Gaus, S.E., Shiromani, P.J. & Saper, C.B. (2002) Selective activation of the extended ventrolateral preoptic nucleus during rapid eye movement sleep. *J. Neurosci.*, **22**, 4568–4576.
Lu, J., Greco, M.A., Shiromani, P. & Saper, C.B. (2000) Effect of lesions of the ventrolateral preoptic nucleus on NREM and REM sleep. *J. Neurosci.*, **20**, 3830–3842.
McGinty, D. & Szymusiak, R. (2000) The sleep–wake switch: a neuronal alarm clark. *Nature Med.*, **6**, 510–511.
Mirmiran, M. & Corner, M. (1982) Neuronal discharge patterns in the occipital cortex of developing rats during active and quiet sleep. *Brain Res.*, **255**, 37–48.
Peyron, C., Tighe, D.K., van den Pol, A.N., de Lecea, L., Heller, H.C., Sutcliffe, J.G. & Kilduff, T.S. (1998) Neurons containing hypocretin (orexin) project to multiple neuronal systems. *J. Neurosci.*, **18**, 9996–10015.
Ramesh, V., Thakkar, M.M., Strecker, R.E., Basheer, R. & McCarley, R.W. (2004) Wakefulness-inducing effects of histamine in the basal forebrain of freely moving rats. *Behav. Brain Res.*, **152**, 271–278.
Saper, C.B., Chou, T.C. & Scammell, T.E. (2001) The sleep switch: hypothalamic control of sleep and wakefulness. *Trends Neurosci.*, **24**, 726–731.
Saper, C.B. & Scammell, T.E. (2004) Modafinil: a drug in search of a mechanism. *Sleep*, **27**, 11–12.
Scammell, T.E., Estabrooke, I.V., McCarthy, M.T., Chemelli, R.M., Yanagisawa, M., Miller, M.S. & Saper, C.B. (2000) Hypothalamic arousal regions are activated during modafinil-induced wakefulness. *J. Neurosci.*, **20**, 8620–8628.
Seelke, A.M.H. & Blumberg, M.S. (2005) Thermal and nutritional modulation of sleep in infant rats. *Behav. Neurosci.*, **19**, 603–611.
Seelke, A.M.H., Karlsson, K.Æ., Gall, A.J. & Blumberg, M.S. (2005) Extraocular muscle activity, rapid eye movements, and the development of active and quiet sleep. *Eur. J. Neurosci.*, **22**, 911–920.
Semba, K. (2000) Multiple output pathways of the basal forebrain: organization, chemical heterogeneity, and roles in vigilance. *Behav. Brain Res.*, **115**, 117–141.
Sherin, J.E., Elmquist, J.K., Torrealba, F. & Saper, C.B. (1998) Innervation of histaminergic tuberomammillary neurons by GABAergic and galaninergic neurons in the ventrolateral preoptic nucleus of the rat. *J. Neurosci.*, **18**, 4705–4721.
Sherin, J.E., Shiromani, P.J., McCarley, R.W. & Saper, C.B. (1996) Activation of ventrolateral preoptic neurons during sleep. *Science*, **271**, 216–219.
Spiers, D.E. & Adair, E.R. (1986) Ontogeny of homeothermy in the immature rat: metabolic and thermal responses. *J. Appl. Physiol.*, **60**, 1190–1197.
Staines, W.A., Daddona, P.E. & Nagy, J.I. (1987a) The organization and hypothalamic projections of the tuberomammillary nucleus in the rat: an immunohistochemical study of adenosine deaminase-positive neurons and fibers. *Neuroscience*, **23**, 571–596.
Staines, W.A., Yamamoto, T., Daddona, P.E. & Nagy, J.I. (1987b) The hypothalamus receives major projections from the tuberomammillary nucleus in rat. *Neurosci. Lett.*, **76**, 257–262.
Steininger, T.L., Gong, H., McGinty, D. & Szymusiak, R. (2001) Subregional organization of preoptic area/anterior hypothalamic projections to arousal-related monoaminergic cell groups. *J. Comp. Neurol.*, **429**, 638–653.
Szymusiak, R. (1995) Magnocellular nuclei of the basal forebrain: substrates of sleep and arousal regulation. *Sleep*, **18**, 478–500.
Szymusiak, R., Alam, N., Steininger, T.L. & McGinty, D. (1998) Sleep–waking discharge patterns of ventrolateral preoptic/anterior hypothalamic neurons in rats. *Brain Res.*, **803**, 178–188.
Szymusiak, R. & McGinty, D. (1986) Sleep-related neuronal discharge in the basal forebrain of cats. *Brain Res.*, **370**, 82–92.
Szymusiak, R. & McGinty, D. (1989) Sleep–waking discharge of basal forebrain projection neurons in cats. *Brain Res. Bull.*, **22**, 423–430.
Willie, J.T., Renthal, W., Chemelli, R.M., Miller, M.S., Scammell, T.E., Yanagisawa, M. & Sinton, C.M. (2005) Modafinil more effectively induces wakefulness in orexin-null mice than in wild-type littermates. *Neuroscience*, **130**, 983–995.
Yang, Q.Z. & Hatton, G.I. (1997) Electrophysiology of excitatory and inhibitory afferents to rat histaminergic tuberomammillary nucleus neurons from hypothalamic and forebrain sites. *Brain Res.*, **773**, 162–172.
Zaborszky, L. & Duque, A. (2003) Sleep–wake mechanisms and basal forebrain circuitry. *Front. Biosci.*, **8**, d1146–d1169.